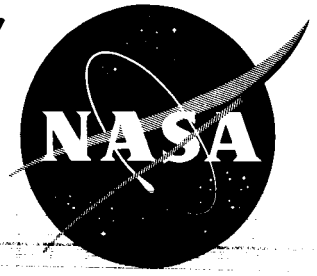

TECHNICAL NOTE

D-652

THEORETICAL EVALUATION OF THE PRESSURES, FORCES, AND MOMENTS AT HYPERSONIC SPEEDS ACTING ON ARBITRARY BODIES OF REVOLUTION UNDERGOING SEPARATE AND COMBINED ANGLE-OF-ATTACK AND PITCHING MOTIONS

By Kenneth Margolis

Langley Research Center
Langley Field, Va.

NATIONAL AERONAUTICS AND SPACE ADMINISTRATION

WASHINGTON

June 1961

NATIONAL AERONAUTICS AND SPACE ADMINISTRATION

TECHNICAL NOTE D-652

THEORETICAL EVALUATION OF THE PRESSURES, FORCES, AND MOMENTS AT HYPERSONIC SPEEDS ACTING ON ARBITRARY BODIES OF REVOLUTION UNDERGOING SEPARATE AND COMBINED ANGLE-OF-ATTACK AND PITCHING MOTIONS

By Kenneth Margolis

SUMMARY

Equations based on Newtonian impact theory have been derived and a computational procedure developed with the aid of several design-type charts which enable the determination of the aerodynamic forces and moments acting on arbitrary bodies of revolution undergoing either separate or combined angle-of-attack and pitching motions. Bodies with axially increasing and decreasing cross-sectional area distributions are considered; nose shapes may be sharp, blunt, or flat faced. The analysis considers variations in angle of attack from -90° to 90° and allows for both positive and negative pitching rates of arbitrary magnitude. The results are also directly applicable to bodies in either separate or combined sideslip and yawing maneuvers.

INTRODUCTION

The purpose of the present paper is to develop a method based primarily on Newtonian impact theory for calculating the aerodynamic forces at hypersonic speeds acting on arbitrary bodies of revolution undergoing either separate or combined angle-of-attack and pitching motions. Bodies with axially decreasing as well as axially increasing cross-sectional area distributions are considered in the analysis. Nose shapes may be sharp, blunt, or flat faced, and forebody shielding effects on flared aft regions are taken into account. The angle-of-attack range considered is $-90^{\circ} \leqq \alpha \leqq 90^{\circ}$ and pitching velocities, both positive and negative, of arbitrary magnitude are allowed. Thus, the formulation of the problem is broad in scope and allows for general application of the results obtained to missiles and aircraft configurations of current interest for a wide range of flight conditions.

Equations are derived and a computational procedure developed with the use of several design-type charts which permit the calculation of the normal and axial forces and pitching moment for any desired body. Some consideration is also given the problem of modifying the results obtained to account for the effects of Mach number variation and differences in the ratio of specific heats.

Although the pitching motion referred to herein is a steady-state effect, it is known that the impact theory when applied to uniformly accelerated motion, that is, $\dot{\alpha}$ effect, predicts a zero resulting force and moment. Therefore, the analysis and results of the present investigation can be considered to include the unsteady pitching condition for low-frequency oscillations. Because of symmetry considerations, the results are also directly applicable to arbitrary bodies of revolution undergoing either separate or combined sideslip and yawing motions, and low-frequency lateral oscillations.

L 1 2 2 5

SYMBOLS

x,r,ω	cylindrical coordinates (see sketch (a))
y,z	rectangular coordinates (see sketch (d))
$R(x)$	body radius in r,ω plane (see sketch (a))
$R'(x)$	axial rate of change of body radius, $\frac{dR(x)}{dx}$
R_o	body radius at nose
R_b	radius of cylindrical section (see sketch (b))
M	Mach number
γ	ratio of specific heats
p	local pressure
p_∞	free-stream pressure
V_∞	free-stream velocity
ρ_∞	free-stream density

C_p coefficient of pressure difference, $\frac{p - p_\infty}{\frac{1}{2}\rho_\infty V_\infty^2}$

α angle of attack

q angular pitching velocity (see sketch (a))

V_N local normal component of resultant velocity

S_r reference area used for nondimensionalizing purposes

l_r reference length used for nondimensionalizing purposes

l body length

C_N normal-force coefficient, $\frac{\text{Normal force}}{\frac{1}{2}\rho_\infty V_\infty^2 S_r}$

C_L lift coefficient, $\frac{\text{Lift}}{\frac{1}{2}\rho_\infty V_\infty^2 S_r}$

C_X axial-force coefficient, $\frac{\text{Axial force}}{\frac{1}{2}\rho_\infty V_\infty^2 S_r}$

C_D drag coefficient, $\frac{\text{Drag}}{\frac{1}{2}\rho_\infty V_\infty^2 S_r}$

C_m pitching-moment coefficient, $\frac{\text{Pitching moment}}{\frac{1}{2}\rho_\infty V_\infty^2 S_r l_r}$

x_o location of pitch axis and moment reference, measured positively rearward from nose (see sketch (a))

$G(x)$ function defined by equation (4)

k maximum percent shielding due to forebody, defined by equation (25)

s maximum cross-sectional periphery at a given axial station shielded by forebody (see sketch (c))

θ	angle subtended by periphery s (see sketch (c))
ω_b	angle used for evaluating forebody-shielding effect, $\lvert\omega_b\rvert = \frac{1}{2}(\pi - \theta)$, (see sketch (c))
l_1, l_2	used as integration limits to denote portion of body length l
$I_1[G(x)]$, $I_2[G(x)]$, $I_3[G(x)]$, $I[G(x)]$	functions associated with evaluation of axial force (see eqs. (10) to (12) and (16) to (18))
$J_1[G(x)]$, $J_2[G(x)]$, $J_3[G(x)]$, $J[G(x)]$	functions associated with evaluation of normal force and pitching moment (see eqs. (13) to (15) and (16) to (18))
ΔC_N, ΔC_X, ΔC_m, $\Delta I[G(x)]$, $\Delta J[G(x)]$	increments or decrements in previously defined quantities
a	parameter used in evaluating flat-faced nose contributions, $\frac{\cos \alpha}{q \frac{R_O}{V_\infty}}$

Superscript:

*	denotes basic contribution plus forebody-shielding effect

Subscripts:

f denotes contribution of flat-faced nose section

t denotes total contributions from all sources

Stability derivatives are discussed in the appendix and are defined therein.

ANALYSIS

The Newtonian impact theory is strictly applicable at Mach numbers approaching infinity and for values of γ, the ratio of specific heats, approaching unity. Studies of this approximate theory and simple modifications thereof (for example, refs. 1 and 2) have shown the Newtonian concept to be a valuable tool in predicting general trends and in many instances yielding quantitative results of acceptable accuracy when applied to high supersonic and hypersonic speeds.

Basically, the theory assumes that the shock wave lies on the body surface and that the flow, upon striking the body, loses all of its momentum in the direction normal to the body surface and continues along the surface with its tangential component of momentum unchanged. Furthermore, only those surface areas under direct impact from the airstream, that is, surface areas which "see" the flow, will experience a pressure force. The Newtonian approximation does not predict any effect on those surface areas facing away or "shielded" from the flow; in these regions the flow is assumed to be completely separated and the local pressure is equal to the free-stream pressure.

The Newtonian hypothesis yields a local pressure coefficient which may be expressed as (see refs. 2 and 3)

$$C_p = \frac{p - p_\infty}{\frac{1}{2}\rho_\infty V_\infty^2} = 2\left(\frac{V_N}{V_\infty}\right)^2 \tag{1}$$

where ρ_∞, p_∞, and V_∞ are the free-stream density, pressure, and velocity, respectively, and where p and V_N are the local pressure and local normal component of resultant velocity, respectively. It is to be noted that equation (1) is applicable only to those surface areas that face the flow; for surface areas that are shielded from the flow, $p = p_\infty$ and $C_p = 0$.

Consider the body of revolution defined with respect to the cylindrical coordinate system shown in the following sketch.

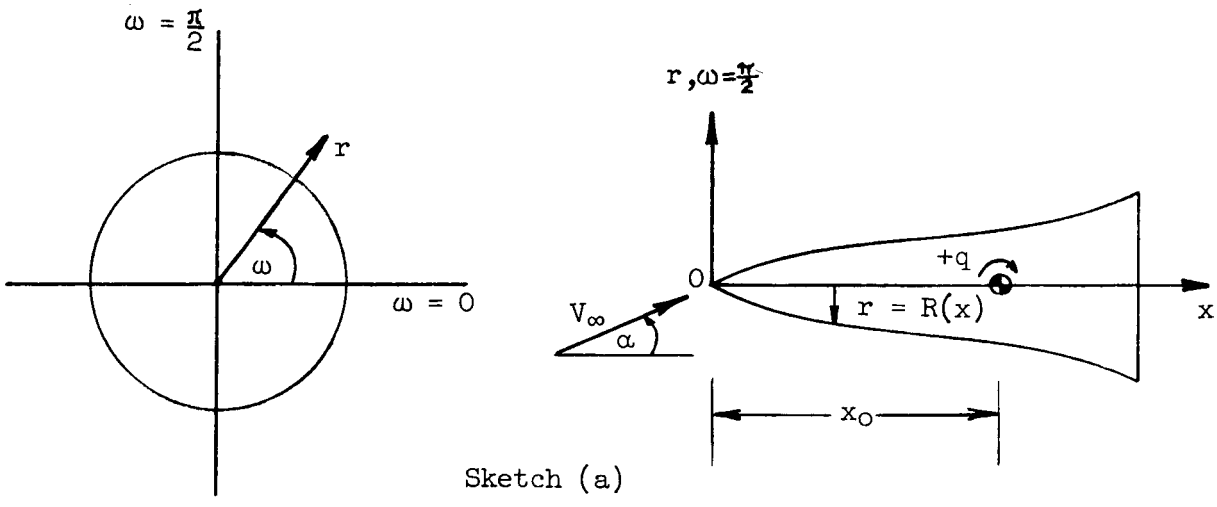

Sketch (a)

The origin is located at the apex or in the case of a body with a flat face, at the intersection of the body axis of symmetry (x-axis) and the face plane. The axis of pitch and moment reference is located at $x = x_o$ measured positively rearward; positive sense of rotation is nose-up as indicated.

The local normal velocity V_N resulting from a combined angle-of-attack and pitching motion $\left(-\frac{\pi}{2} \leqq \alpha \leqq \frac{\pi}{2};\ -\infty < q < \infty\right)$ applicable to surface areas that are subject to compression flow, that is, that "see" the flow has been derived (refs. 3 and 4) and is expressible in the following form:

$$V_N(\omega,x) = \frac{V_\infty \cos\alpha}{\sqrt{1 + R'^2(x)}}\left\{R'(x) - \tan\alpha \sin\omega - \frac{q \sin\omega}{V_\infty \cos\alpha}\left[x - x_o + R(x)R'(x)\right]\right\} \tag{2}$$

where $R(x)$ and $R'(x)$ define the body shape and its rate of change with axial distance.

Substitution of equation (2) into equation (1) yields the local pressure coefficient

$$C_p(\omega,x) = \frac{2}{1 + R'^2(x)}\left\{R'^2(x)\cos^2\alpha - R'(x)\sin\omega\sin 2\alpha + \sin^2\omega\sin^2\alpha \right.$$

$$- 2\frac{q}{V_\infty}\sin\omega\cos\alpha R'(x)\left[R(x)R'(x) + x - x_o\right]$$

$$+ 2\frac{q}{V_\infty}\sin^2\omega\sin\alpha\left[R(x)R'(x) + x - x_o\right]$$

$$\left. + \left(\frac{q}{V_\infty}\right)^2\sin^2\omega\left[R(x)R'(x) + x - x_o\right]^2\right\} \qquad (3)$$

Considerable simplification is afforded by use of the substitution

$$G(x) = \frac{\frac{q}{V_\infty}\left[R(x)R'(x) + x - x_o\right] + \sin\alpha}{R'(x)\cos\alpha} \qquad (4)$$

which enables equation (3) to be rewritten as follows:

$$C_p(\omega,x) = \frac{2R'^2(x)\cos^2\alpha}{1 + R'^2(x)}\left[G^2(x)\sin^2\omega - 2G(x)\sin\omega + 1\right]$$

or

$$C_p(\omega,x) = \frac{2R'^2(x)\cos^2\alpha}{1 + R'^2(x)}\left[1 - G(x)\sin\omega\right]^2 \qquad (5)$$

where $G(x)\sin\omega \leqq 1$ for $R'(x) \geqq 0$ and where $G(x)\sin\omega \geqq 1$ for $R'(x) < 0$. The conditions on $G(x)\sin\omega$ insure that the surface region under consideration is not shielded from the flow. When the surface is shielded, i.e., $G(x)\sin\omega > 1$ for $R'(x) > 0$ or $G(x)\sin\omega < 1$ for $R'(x) < 0$, $C_p(\omega,x)$ is, of course, zero. An examination of equation (2) in conjunction with the substitution of equation (4) and the requirement that $V_N \geqq 0$ readily yields the indicated inequalities. It should be noted that, for $R'(x) = 0$, the parameter $G(x)$ is infinite and a more convenient expression for the pressure coefficient $C_p(\omega,x)$ is directly obtainable from equation (3).

When the body of revolution has a flat circular face, the face pressure predicted by the Newtonian theory may be obtained from equation (5) by the following substitutions therein: $x = 0$, $R(x) = r$, $R'(x) \to \infty$, and $G(x) = \dfrac{qr}{V_\infty \cos \alpha}$. The formula for this pressure is given in coefficient form by:

$$C_{p,f} = 2 \cos^2\alpha \left(1 - \frac{qr}{V_\infty \cos \alpha} \sin \omega\right)^2 \tag{6}$$

and is applicable to those regions that are not shielded from the flow, i.e., $r \sin \omega \leqq \dfrac{V_\infty \cos \alpha}{q}$. For shielded regions, i.e., $r \sin \omega > \dfrac{V_\infty \cos \alpha}{q}$, $C_{p,f}$ is zero.

Another effect that requires consideration is the shielding of flared aft regions of the body due to the presence of the forebody. For example, the lateral surface area of a conical frustum would be completely exposed to the flow at a sufficiently small α and for $q = 0$ if the frustum was used as the forward section of a body; if, however, the same frustum was positioned as a flared aft section behind a cylindrical midsection, then part of the frustum would be shielded from the flow. A later section of the paper treats the problem of estimating corrections to the calculated forces and moments so as to account for such shielding effects.

In the calculation of the axial force, normal force, and pitching moment for an arbitrary body of revolution, there are therefore three components to be considered: (a) the basic forces and moments associated with the body, exclusive of forebody shielding effects; (b) corrections necessitated by forebody shielding effects; and (c) the contribution of a flat-faced nose shape.

The basic forces and moments (item (a) above) may be expressed in the following manner:

$$C_N = -\frac{2}{S_r} \int_0^l \int_{\omega_1(x)}^{\omega_2(x)} R(x) C_p(\omega, x) \sin \omega \, d\omega \, dx \tag{7}$$

$$C_X = \frac{2}{S_r} \int_0^{l} \int_{\omega_1(x)}^{\omega_2(x)} R(x)R'(x)C_p(\omega,x)d\omega\, dx \tag{8}$$

$$C_m = \frac{2}{S_r l_r} \int_0^{l} \int_{\omega_1(x)}^{\omega_2(x)} R(x)\left[R(x)R'(x) + x - x_o\right]C_p(\omega,x)\sin\omega\, d\omega\, dx \tag{9}$$

where l is the overall body length, S_r and l_r are the reference area and reference length, respectively, used for nondimensionalizing purposes, and functions $\omega_1(x)$ and $\omega_2(x)$ are the ω limits determined by the $V_N = 0$ velocity boundary and the applicable range of ω, i.e., $-\frac{\pi}{2} \leqq \omega \leqq \frac{\pi}{2}$. Because of symmetry considerations, the multiplicative factor of 2 accounts for the forces and moments acting on the complete body.

For body regions that are completely exposed to the flow, $\omega_1(x) = -\frac{\pi}{2}$ and $\omega_2(x) = \frac{\pi}{2}$; for body regions where part of the lower surface is shielded, $\omega_1(x) = \text{arc csc } G(x)$ and $\omega_2 = \frac{\pi}{2}$; and for body regions where part of the upper surface is shielded, $\omega_1(x) = -\frac{\pi}{2}$ and $\omega_2(x) = \text{arc csc } G(x)$. Inasmuch as the calculations of C_N, C_X, and C_m involve (see eqs. (7) to (9)) integrations with respect to the variable ω of the quantities $C_p(\omega,x)$ and $C_p(\omega,x)\sin\omega$, it is convenient to define the following functions of $G(x)$:

$$I_1\left[G(x)\right] = \int_{\text{arc csc } G(x)}^{\pi/2} C_p(\omega,x)d\omega \qquad \begin{pmatrix} R'(x) \geqq 0: & G(x) < -1 \\ R'(x) < 0: & G(x) \geqq 1 \end{pmatrix} \tag{10}$$

$$I_2\left[G(x)\right] = \int_{-\pi/2}^{\pi/2} C_p(\omega,x)d\omega \qquad \left(R'(x) > 0: \quad -1 \leqq G(x) \leqq 1\right) \tag{11}$$

$$I_3\left[G(x)\right] = \int_{-\pi/2}^{\text{arc csc } G(x)} C_p(\omega,x)d\omega \qquad \begin{pmatrix} R'(x) \geqq 0: & G(x) > 1 \\ R'(x) < 0: & G(x) \leqq -1 \end{pmatrix} \tag{12}$$

$$J_1[G(x)] = \int_{\text{arc csc } G(x)}^{\pi/2} C_p(\omega,x)\sin\omega\, d\omega \qquad \begin{pmatrix} R'(x) \geqq 0: & G(x) < -1 \\ R'(x) < 0: & G(x) \geqq 1 \end{pmatrix} \quad (13)$$

$$J_2[G(x)] = \int_{-\pi/2}^{\pi/2} C_p(\omega,x)\sin\omega\, d\omega \qquad \left(R'(x) > 0: \quad -1 \leqq G(x) \leqq 1\right) \quad (14)$$

$$J_3[G(x)] = \int_{-\pi/2}^{\text{arc csc } G(x)} C_p(\omega,x)\sin\omega\, d\omega \qquad \begin{pmatrix} R'(x) \geqq 0: & G(x) > 1 \\ R'(x) < 0: & G(x) \leqq -1 \end{pmatrix} \quad (15)$$

where the ranges of $R'(x)$ and $G(x)$ variations are indicated parenthetically next to each integral.

Upon integration, and designation of the various I and J functions as simply $I[G(x)]$ and $J[G(x)]$, the following formulas and relations result:

For $0 \leqq G(x) \leqq 1$ and $R'(x) > 0$,

$$\left.\begin{aligned} \frac{1 + R'^2(x)}{R'^2(x)} \sec^2\alpha\, I[G(x)] &= \pi[G^2(x) + 2] \\ \frac{1 + R'^2(x)}{R'^2(x)} \sec^2\alpha\, J[G(x)] &= -2\pi G(x) \end{aligned}\right\} \quad (16)$$

For $G(x) > 1$ and $R'(x) > 0$ or for $G(x) \leqq -1$ and $R'(x) < 0$,

$$\left.\begin{aligned} \frac{1 + R'^2(x)}{R'^2(x)} \sec^2\alpha\, I[G(x)] &= [2 + G^2(x)]\,\text{arc sec-}G(x) + 3\frac{G(x)}{|G(x)|}\sqrt{G^2(x) - 1} \\ \frac{1 + R'^2(x)}{R'^2(x)} \sec^2\alpha\, J[G(x)] &= -2G(x)\,\text{arc sec-}G(x) - \frac{4G^2(x) + 2}{3|G(x)|}\sqrt{G^2(x) - 1} \end{aligned}\right\} \quad (17)$$

For $G(x) < 0$ and $R'(x) > 0$ or for $G(x) \geq 1$ and $R'(x) < 0$,

$$\left.\begin{aligned} I\left[G(x)\right] &= I\left[-G(x)\right] \\ J\left[G(x)\right] &= -J\left[-G(x)\right] \end{aligned}\right\} \tag{18}$$

It should be noted that, for $R'(x) < 0$ and $-1 < G(x) < 1$, the surface region is shielded from the flow $\left(C_p(\omega,x) = 0\right)$ and therefore both $I\left[G(x)\right]$ and $J\left[G(x)\right]$ are zero. For the special cases where $G(x) \to \pm\infty$, a condition which arises when $R'(x) = 0$ and/or $|\alpha| = \frac{\pi}{2}$, the following formulas are applicable:

For $G(x) \to \pm\infty$ and $R'(x) = 0$,

$$\left.\begin{aligned} I\left[G(x)\right] &= \frac{\pi}{2}\left[\frac{q}{V_\infty}(x - x_o) + \sin\alpha\right]^2 \\ J\left[G(x)\right] &= \mp\frac{4}{3}\left[\frac{q}{V_\infty}(x - x_o) + \sin\alpha\right]^2 \end{aligned}\right\} \tag{19}$$

For $G(x) \to \pm\infty$, $|\alpha| = \frac{\pi}{2}$, and $R'(x) > 0$ or for $G(x) \to \mp\infty$, $|\alpha| = \frac{\pi}{2}$, and $R'(x) < 0$,

$$\left.\begin{aligned} I\left[G(x)\right] &= \frac{\pi}{2\left[1 + R'^2(x)\right]}\left\{\frac{q}{V_\infty}\left[R(x)R'(x) + x - x_o\right] + \frac{\alpha}{|\alpha|}\right\}^2 \\ J\left[G(x)\right] &= \mp\frac{4}{3\left[1 + R'^2(x)\right]}\left\{\frac{q}{V_\infty}\left[R(x)R'(x) + x - x_o\right] + \frac{\alpha}{|\alpha|}\right\}^2 \end{aligned}\right\} \tag{20}$$

Equations (7) to (9) may be rewritten in terms of the $I\left[G(x)\right]$ and $J\left[G(x)\right]$ functions:

$$C_N = -\frac{2}{S_r}\int_0^l R(x)\, J\left[G(x)\right] dx \tag{21}$$

$$C_X = \frac{2}{S_r} \int_0^l R(x)R'(x)\, I\left[G(x)\right] dx \tag{22}$$

$$C_m = \frac{2}{S_r l_r} \int_0^l R(x)\left[R(x)R'(x) + x - x_o\right] J\left[G(x)\right] dx \tag{23}$$

For any given body, therefore, the integrands of equations (21) to (23) may readily be computed for various x-stations and a simple graphical or numerical integration performed to yield the forces and moments. In order to facilitate such calculations, design-type charts for the $I\left[G(x)\right]$ and $J\left[G(x)\right]$ functions, computed from equations (16) to (18), are presented in figures 1 and 2, respectively, which are contained in a pocket attached to the back cover of this report.

The second component to be considered in the force and moment calculations is (item (b)) the correction necessitated by forebody shielding effects if applicable to the given body for the specified angle of attack and pitching velocity. In this connection, it should be noted that an exact correction would be a function of many variables and thus would not be useful as a simple design-type procedure. It is also felt that for most bodies this particular effect is not too significant overall and thus a calculation to define the maximum correction possible for a simple shape would be more appropriate.

Consider, then, a flared aft section situated behind an infinite circular cylinder of radius R_b shown in the following sketch:

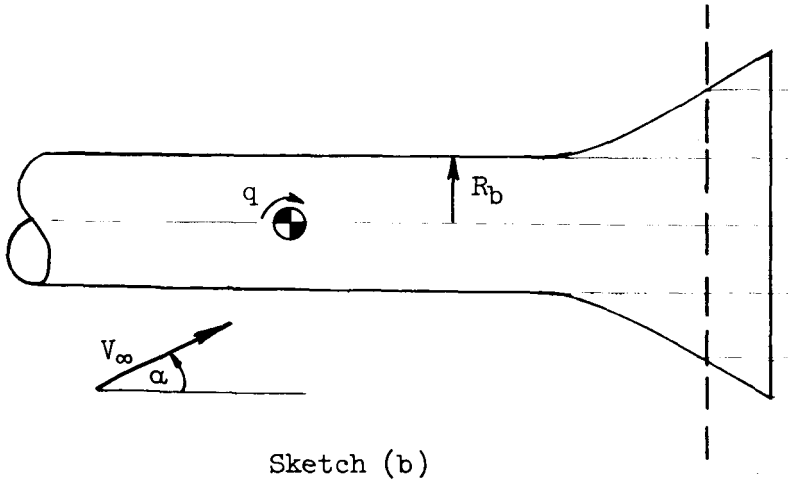

Sketch (b)

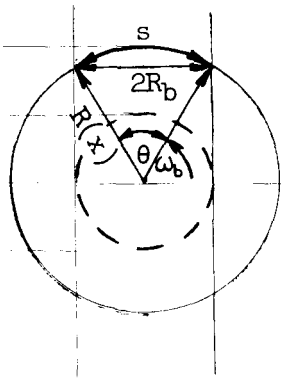

Sketch (c)

At an axial location x behind the cylinder, the maximum cross-sectional periphery shielded by the cylinder is s (see sketch (c)) where

$$s = \theta R(x) = R(x)\arccos\left[1 - 2\left(\frac{R_b}{R(x)}\right)^2\right]$$

or by trigonometric substitution,

$$s = 2R(x)\arccos\sqrt{1 - \left(\frac{R_b}{R(x)}\right)^2} \tag{24}$$

The quantity $\frac{s}{2\pi R(x)}$ expresses the maximum percent shielding that may be present due to the forebody. The following relation exists:

$$\frac{s}{2\pi R(x)} = k = \frac{100}{\pi}\arccos\sqrt{1 - \left(\frac{R_b}{R(x)}\right)^2} \tag{25}$$

and it is readily apparent that the maximum percent shielding ranges from 0 $\left(\frac{R_b}{R(x)} = 0\right)$ to 50 percent $\left(\frac{R_b}{R(x)} = 1\right)$. The variation of the parameter k with the ratio $\frac{R_b}{R(x)}$ is shown in figure 3.

The parameter k may in turn be related to the integration limit ω_b

$$k = \frac{2R(x)\left(\frac{\pi}{2} - \omega_b\right)}{2\pi R(x)} \times 100 = 50 - \frac{100}{\pi}\omega_b \tag{26}$$

where

$$\omega_b = \arcsin\sqrt{1 - \left(\frac{R_b}{R(x)}\right)^2} \tag{27}$$

Omitting calculation details, the procedure is to derive expressions for $\Delta I\left[G(x)\right]$ and $\Delta J\left[G(x)\right]$ through use of equations (10), (12), (13), and (15) with appropriate changes in the ω limits of integration so as to account for the shielding boundary ω_b. Corresponding corrections to the force and moment are then introduced:

$$\left.\begin{aligned} C_N^* &= C_N + \Delta C_N \\ C_X^* &= C_X + \Delta C_X \\ C_m^* &= C_m + \Delta C_m \end{aligned}\right\} \qquad (28)$$

L
1
2
2
5

where

$$\Delta C_X = -\frac{2}{S_r}\int_{l_1}^{l_2} R(x)R'(x)\,\Delta I\left[G(x)\right]dx \qquad (29)$$

$$\Delta C_N = -\frac{2}{S_r}\int_{l_1}^{l_2} R(x)\,\Delta J\left[G(x)\right]dx \qquad (30)$$

and

$$\Delta C_m = \frac{2}{S_r l_r}\int_{l_1}^{l_2} R(x)\left[R(x)R'(x) + x - x_o\right]\Delta J\left[G(x)\right]dx \qquad (31)$$

In equations (29) to (31), the integration is performed over that section of body length affected by the forebody, herein denoted from l_1 to l_2. The functions $\Delta I\left[G(x)\right]$ and $\Delta J\left[G(x)\right]$ are tabulated as follows:

For $0 \leqq G(x) \leqq 1$ and $0 \leqq \omega_b \leqq \frac{\pi}{2}$,

$$\left.\begin{aligned}
\frac{1 + R'^2(x)}{R'^2(x)} \sec^2\alpha \, \Delta I\left[G(x)\right] &= G^2(x)\left(\frac{\pi}{2} - \omega_b + \cos\omega_b \sin\omega_b\right) \\
&\quad - 4G(x)\cos\omega_b + \pi - 2\omega_b \\
\frac{1 + R'^2(x)}{R'^2(x)} \sec^2\alpha \, \Delta J\left[G(x)\right] &= -2\left[\frac{G^2(x)\cos\omega_b\left(2 + \sin^2\omega_b\right)}{3}\right. \\
&\quad \left. + G(x)\left(\omega_b - \cos\omega_b \sin\omega_b - \frac{\pi}{2}\right) + \cos\omega_b\right]
\end{aligned}\right\} \tag{32}$$

For $1 \leqq G(x) < \infty$ and $0 \leqq \omega_b \leqq \text{arc csc } G(x)$

$$\left.\begin{aligned}
\frac{1 + R'^2(x)}{R'^2(x)} \sec^2\alpha \, \Delta I\left[G(x)\right] &= \left[G^2(x) + 2\right]\text{arc sec-}G(x) \\
&\quad + 3\sqrt{G^2(x) - 1} - 4G(x)\cos\omega_b \\
&\quad + G^2(x)\left(\cos\omega_b \sin\omega_b - \frac{\pi}{2} - \omega_b\right) - 2\omega_b - \pi \\
\frac{1 + R'^2(x)}{R'^2(x)} \sec^2\alpha \, \Delta J\left[G(x)\right] &= -2\left[\cos\omega_b + G(x)\left(\frac{\pi}{2} + \omega_b - \cos\omega_b \sin\omega_b\right)\right. \\
&\quad + \frac{G^2(x)\cos\omega_b\left(2 + \sin^2\omega_b\right)}{3} \\
&\quad - \frac{2G^2(x) + 1}{3G(x)}\sqrt{G^2(x) - 1} \\
&\quad \left. - G(x)\text{arc sec-}G(x)\right]
\end{aligned}\right\} \tag{33}$$

For $-1 \leqq G(x) < 0$ and $-\frac{\pi}{2} \leqq \omega_b \leqq 0$, or $-\infty < G(x) < -1$ and $\arccsc G(x) \leqq \omega_b \leqq 0$,

$$\left.\begin{aligned} \Delta I\left[-G(x)\right] &= \Delta I\left[G(x)\right] \\ \Delta J\left[-G(x)\right] &= -\Delta J\left[G(x)\right] \end{aligned}\right\} \tag{34}$$

For any other combinations of the parameters ω_b and $G(x)$, the forebody does not give rise to any additional shielding and the correction factors are zero, that is, $\Delta I\left[G(x)\right] = 0$ and $\Delta J\left[G(x)\right] = 0$. The variations of $\Delta I\left[G(x)\right]$ and $\Delta J\left[G(x)\right]$ with the parameter $G(x)$ are shown in figures 4 and 5 for several values of maximum percent shielding. Included in these figures are the basic $I\left[G(x)\right]$ and $J\left[G(x)\right]$ curves so that the relative importance of the corrections can be assessed. The corrections ΔC_N, ΔC_X, and ΔC_m may now be readily obtained for any given body in accordance with equations (29) to (31) by using the identical procedure discussed previously for calculating C_N, C_X, and C_m.

Although the corrections $\Delta I\left[G(x)\right]$ and $\Delta J\left[G(x)\right]$ just discussed are directly applicable to flared aft sections situated behind forebodies for which $R'(x) \geqq 0$, a similar approach utilizing an average or modified value of R_b could readily be applied (if required) to body shapes with regions characterized by $R'(x) < 0$.

In the event the body of revolution considered has a flat face, a third contribution (item (c)) to the force and moments is involved. The incremental normal force will, of course, be zero but the axial-force and pitching-moment increments will be finite.

The pressure acting on the flat face is given by equation (6) as

$$C_{p,f} = 2 \cos^2\alpha\left(1 - \frac{qr}{V_\infty \cos \alpha} \sin \omega\right)^2$$

Consider the following sketch:

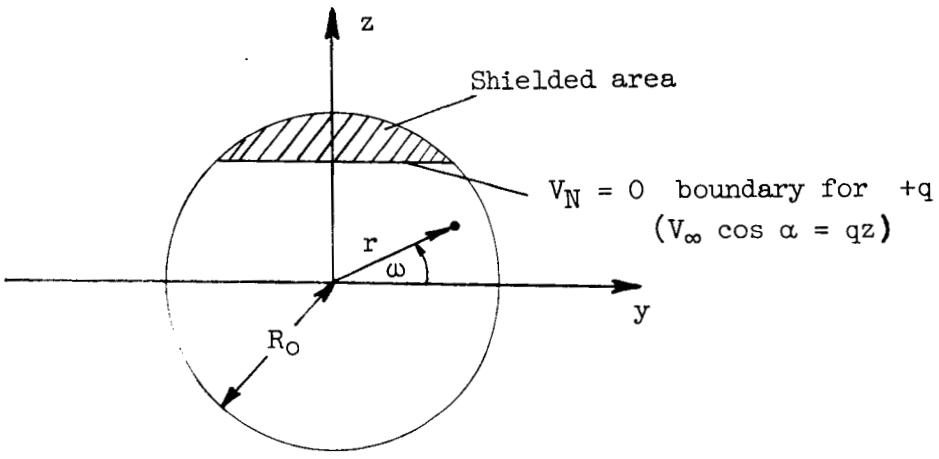

Sketch (d)

If, for convenience, the parameter a is introduced to denote the quantity $\frac{\cos \alpha}{q \frac{R_o}{V_\infty}}$, it is readily seen that no shielding effects will be present for values of $|a| \geq 1$ and the following integral expressions may be written:

$$C_{X,f} = \frac{4 \cos^2\alpha}{S_r} \int_{-R_o}^{R_o} \int_{0}^{\sqrt{R_o^2 - z^2}} \left(1 - \frac{z}{aR_o}\right)^2 dy\, dz \tag{35}$$

$$C_{m,f} = \frac{4 \cos^2\alpha}{S_r l_r} \int_{-R_o}^{R_o} \int_{0}^{\sqrt{R_o^2 - z^2}} \left(1 - \frac{z}{aR_o}\right)^2 z\, dy\, dz \tag{36}$$

For values of $|a| < 1$, the equations above apply provided the following changes in limits are incorporated to account for the shielding boundary: for $q > 0$, replace upper limit on z by aR_o, and for $q < 0$, replace lower limit on z by aR_o.

The indicated operations have been carried out and the following closed-form formulas result:

For $|a| \geqq 1$,

$$\left.\begin{aligned} C_{N,f} &= 0 \\ C_{X,f} &= \frac{\pi R_o^2 \cos^2\alpha}{S_r} \frac{1 + 4a^2}{2a^2} \\ C_{m,f} &= -\frac{\pi R_o^3 \cos^2\alpha}{S_r l_r} \frac{1}{a} \end{aligned}\right\} \tag{37}$$

L 1225

For $|\bar{a}| < 1$,

$$\left.\begin{aligned} C_{N,f} &= 0 \\ C_{X,f} &= \frac{R_o^2 \cos^2\alpha}{S_r} \frac{3(4a^2 + 1)\arccos|a| + |a|(2a^2 + 13)\sqrt{1 - a^2}}{6a^2} \\ C_{m,f} &= -\frac{R_o^3 \cos^2\alpha}{S_r l_r} \frac{15a \arccos|a| - \frac{a}{|a|}\left(2a^4 - 9a^2 - 8\right)\sqrt{1 - a^2}}{15a^2} \end{aligned}\right\} \tag{38}$$

The variations of $C_{X,f}$ and $C_{m,f}$ with the parameter a are shown in figure 6. It should be noted that only positive values of a need be considered since $C_{X,f}(a) = C_{X,f}(-a)$, and $C_{m,f}(a) = -C_{m,f}(-a)$.

Thus the three contributions to the forces and moments have been considered: (a) the basic components C_N, C_X, C_m, (b) the forebody shielding components ΔC_N, ΔC_X, ΔC_m, and (c) the flat-face contributions $C_{N,f}$, $C_{X,f}$, $C_{m,f}$. These components are additive,

$$\left.\begin{aligned} C_{N,t} &= C_N + \Delta C_N + C_{N,f} \\ C_{X,t} &= C_X + \Delta C_X + C_{X,f} \\ C_{m,t} &= C_m + \Delta C_m + C_{m,f} \end{aligned}\right\} \tag{39}$$

In the event the lift coefficient C_L and drag coefficient C_D are desired, they may readily be obtained by the formulas:

$$\left.\begin{aligned} C_L &= C_N \cos \alpha - C_X \sin \alpha \\ C_D &= C_N \sin \alpha + C_X \cos \alpha \end{aligned}\right\} \tag{40}$$

L
1
2
2
5

For values of α and q in the immediate vicinity of zero, a convenient form for evaluating stability derivatives may be obtained from the equations derived herein; they are presented for general interest in the appendix.

APPLICATION OF METHOD

In order to illustrate the procedures used in evaluating the aerodynamic forces and moments, consider the body of revolution shown in figure 7 consisting of a hemispherical nose faired into a cylindrical midsection followed by a flared aft region composed of two conical frustums. The equations defining body shape and slope are given in the figure along with values chosen for aerodynamic parameters (angle of attack $\alpha = 20^\circ$, positive pitching $\frac{q}{V_\infty} = 0.015$ about center of gravity $\frac{x_o}{l} = \frac{4}{9}$). For purposes of convenience, the body length is chosen as 9 units and the corresponding lengths of other quantities are indicated.

Sufficient axial stations are chosen (21, indicated by the dots along the body axis of symmetry) and a value of $G(x)$ computed from equation (4) for each value of x. For each $G(x)$ value so obtained, there are read off from figures 1 and 2, respectively, values of the $I\left[G(x)\right]$ and $J\left[G(x)\right]$ parameters. (For values of $G(x) \to \infty$, simple computations are made directly from the formulas included in the figures.) Then in accordance with equations (21), (22), and (23) the functions $R(x)\cdot J\left[G(x)\right]$, $R(x)\cdot R'(x)\cdot I\left[G(x)\right]$, and $R(x)\cdot\left[R(x)R'(x) + x - x_o\right]\cdot J\left[G(x)\right]$ are tabulated and plotted against the axial coordinate x as shown in figure 8. Integration by any suitable means (Simpson's Rule, planimeter, etc.) to obtain the areas under the solid-line curves of

figure 8 and multiplication by the appropriate factors of equations (21), (22), and (23) yield the following results for the basic forces and moments:

$$\left.\begin{aligned} C_X &= 0.74 \\ C_N &= 0.54 \\ C_m &= -0.33 \end{aligned}\right\} \tag{41}$$

To calculate the correction due to forebody shielding, that is, ΔC_X, ΔC_N, and ΔC_m, values of the parameter k defined by equation (25) are obtained from figure 3 for those axial stations behind the cylindrical section. The parameters $\Delta I\left[G(x)\right]$ and $\Delta J\left[G(x)\right]$ are then estimated from figures (4) and (5), respectively, and the calculation of the incremental forces and moment defined by equations (29), (30), and (31) proceeds in a manner directly analogous to the procedure described above for the basic contributions. The incremental effects are shown as dashed lines in figure 8 and result in the following corrections:

$$\left.\begin{aligned} \Delta C_X &= -0.03 \\ \Delta C_N &= 0.03 \\ \Delta C_m &= -0.02 \end{aligned}\right\} \tag{42}$$

Inasmuch as the body chosen for illustrative calculations does not have a flat surface at the nose, the flat-face contributions (eqs. (37) and (38)) are, of course, zero. Thus in accordance with equations (28) and (39), the total coefficients are:

$$\left.\begin{aligned} C_{X,t} &= 0.71 \\ C_{N,t} &= 0.57 \\ C_{m,t} &= -0.35 \end{aligned}\right\} \tag{43}$$

It should be noted that the Newtonian theory does not account for either variations in Mach number or for differences in the value of γ, the ratio of specific heats. The theory is strictly valid at Mach numbers approaching infinity and for $\gamma = 1$. Simple modifications to the Newtonian theory have been suggested to account for these variations. As an example for blunt bodies, the Newtonian coefficient might be multiplied by the ratio (see ref. 5), $\frac{\gamma + 3}{2(\gamma + 1)}\left[1 - \frac{2}{(\gamma + 3)M^2}\right]$. For pointed bodies with attached shocks, the Newtonian values appear to be more satisfactory. Some discussion pertinent to Newtonian theory modifications may be found in reference 6.

L
1
2
2
5

CONCLUDING REMARKS

Equations based on Newtonian impact theory have been derived and a computational procedure developed which enables the determination of the aerodynamic forces and moments acting on arbitrary bodies of revolution undergoing either separate or combined angle-of-attack and pitching motions. The analysis considers variations in angle of attack from -90° to 90° and allows for both positive and negative pitching velocities of arbitrary magnitude. The results are also directly applicable to bodies in either separate or combined sideslip and yawing maneuvers.

Langley Research Center,
National Aeronautics and Space Administration,
Langley Field, Va., October 28, 1960.

APPENDIX

CALCULATION OF STABILITY DERIVATIVES

Although the Newtonian theory predicts forces and moments that are nonlinear with respect to variations in angle of attack and/or pitching velocity, considerable attention has been given the problem of calculating stability derivatives, that is, rates of change of forces and moments expressed in nondimensional form (for example, refs. 3 and 7). Inasmuch as the derivatives are conventionally evaluated as $\alpha \to 0$ and $q \to 0$, it is apparent that considerable caution must be exercised in the application of results so obtained without regard to nonlinear effects.

The equations for the basic forces and moments derived in the present paper may be readily expressed in the form of stability derivatives by appropriate differentiation of equations (7), (8), and (9) with the limits $\omega_1(x)$ and $\omega_2(x)$ therein replaced by $-\pi/2$ and $\pi/2$, respectively, and utilization of the evaluations for $I_2\left[G(x)\right]$ and $J_2\left[G(x)\right]$ as given by equation (16). The following formulas result:

$$C_{N_\alpha} = \left(\frac{\partial C_N}{\partial \alpha}\right)_{\substack{\alpha \to 0 \\ q \to 0}} = \frac{4\pi}{S_r} \int_0^l \frac{R(x)R'(x)}{1 + R'^2(x)}\, dx \tag{A1}$$

$$C_{N_q} = \left(\frac{\partial C_N}{\partial \frac{q l_r}{2V_\infty}}\right)_{\substack{q \to 0 \\ \alpha \to 0}} = \frac{8\pi}{S_r l_r} \int_0^l \frac{R(x)R'(x)\left[R(x)R'(x) + x - x_o\right]}{1 + R'^2(x)}\, dx \tag{A2}$$

$$C_{m_\alpha} = \left(\frac{\partial C_m}{\partial \alpha}\right)_{\substack{\alpha \to 0 \\ q \to 0}} = -\frac{4\pi}{S_r l_r} \int_0^l \frac{R(x)R'(x)\left[R(x)R'(x) + x - x_o\right]}{1 + R'^2(x)}\, dx \tag{A3}$$

$$C_{m_q} = \left(\frac{\partial C_m}{\partial \frac{q l_r}{2V_\infty}}\right)_{\substack{q \to 0 \\ \alpha \to 0}} = -\frac{8\pi}{S_r l_r^2} \int_0^l \frac{R(x)R'(x)\left[R(x)R'(x) + x - x_o\right]^2}{1 + R'^2(x)}\, dx \qquad (A4)$$

$$C_{X_\alpha} = \left(\frac{\partial C_X}{\partial \alpha}\right)_{\substack{\alpha \to 0 \\ q \to 0}} = 0 \qquad (A5)$$

$$C_{X_q} = \left(\frac{\partial C_X}{\partial \frac{q l_r}{2V_\infty}}\right)_{\substack{q \to 0 \\ \alpha \to 0}} = 0 \qquad (A6)$$

At the limit $\alpha = 0$ and/or $q = 0$, the normal-force coefficient C_N and the pitching-moment coefficient C_m are both zero, but the axial-force coefficient C_X is finite. A formula for C_X may be derived through use of equations (8) and (16) and is given by

$$\left(C_X\right)_{\substack{\alpha=0 \\ q=0}} = \frac{4\pi}{S_r} \int_0^l \frac{R(x)R'^3(x)}{1 + R'^2(x)}\, dx \qquad (A7)$$

Equations (A1) to (A7) are valid for arbitrary bodies of revolution and may be readily evaluated by analytical, numerical, or graphical procedures.

In the event the body under consideration has a flat face at the nose, there are some additional contributions to be considered; these may be obtained by straightforward differentiations of equations (37) and are as follows:

$$\left(C_{N_\alpha}\right)_f = \left(\frac{\partial C_{N,f}}{\partial \alpha}\right)_{\substack{\alpha \to 0 \\ q \to 0}} = 0 \tag{A8}$$

$$\left(C_{N_q}\right)_f = \left(\frac{\partial C_N}{\partial \frac{q l_r}{2V_\infty}}\right)_{\substack{q \to 0 \\ \alpha \to 0}} = 0 \tag{A9}$$

$$\left(C_{m_\alpha}\right)_f = \left(\frac{\partial C_{m,f}}{\partial \alpha}\right)_{\substack{\alpha \to 0 \\ q \to 0}} = 0 \tag{A10}$$

$$\left(C_{m_q}\right)_f = \left(\frac{\partial C_{m,f}}{\partial \frac{q l_r}{2V_\infty}}\right)_{\substack{q \to 0 \\ \alpha \to 0}} = -\frac{2\pi R_o^{\,4}}{S_r l_r^{\,2}} \tag{A11}$$

$$\left(C_{X_\alpha}\right)_f = \left(\frac{\partial C_{X,f}}{\partial \alpha}\right)_{\substack{\alpha \to 0 \\ q \to 0}} = 0 \tag{A12}$$

$$\left(C_{X_q}\right)_f = \left(\frac{\partial C_{X,f}}{\partial \frac{q l_r}{2V_\infty}}\right)_{\substack{q \to 0 \\ \alpha \to 0}} = 0 \tag{A13}$$

where R_o is the radius at the nose.

At the limit $\alpha = 0$ and/or $q = 0$, the normal-force coefficient $C_{N,f}$ and the pitching-moment coefficient $C_{m,f}$ are both zero, but the axial-force coefficient is finite and is obtained from equation (37) as

$$\left(C_{X,f}\right)_{\substack{\alpha=0 \\ q=0}} = \frac{2\pi R_o^2}{S_r} \tag{A14}$$

Additional increments due to forebody shielding have not been considered; these effects are felt to be relatively insignificant for values of α and q at or in the immediate vicinity of zero. The effects of centrifugal forces in the flow have also been excluded in the analysis.

In the event stability derivatives are desired for values of α and/or q significantly different from zero, it is suggested that force and moment variations with α and q be obtained by the method of the present paper so as to emphasize any nonlinear characteristics. The required slopes may then be estimated by the usual procedures.

REFERENCES

1. Ehret, Dorris M.: Accuracy of Approximate Methods for Predicting Pressures on Pointed Nonlifting Bodies of Revolution in Supersonic Flow. NACA TN 2764, 1952.

2. Grimminger, G., Williams, E. P., and Young, G. B. W.: Lift on Inclined Bodies of Revolution in Hypersonic Flow. Jour. Aero. Sci., vol. 17, no. 11, Nov. 1950, pp. 675-690.

3. Tobak, Murray, and Wehrend, William R.: Stability Derivatives of Cones at Supersonic Speeds. NACA TN 3788, 1956.

4. Charwat, A. F.: The Stability of Bodies of Revolution at Very High Mach Numbers. Jet Propulsion, vol. 27, no. 8, pt. 1, Aug. 1957, pp. 866-871.

5. Rainey, Robert W.: Working Charts for Rapid Prediction of Force and Pressure Coefficients on Arbitrary Bodies of Revolution By Use of Newtonian Concepts. NASA TN D-176, 1959.

6. Lees, Lester: Hypersonic Flow. Preprint No. 554, S.M.F. Fund Preprint, Inst. Aero. Sci, Inc., June 1955.

7. Fisher, Lewis R.: Equations and Charts for Determining the Hypersonic Stability Derivatives of Combinations of Cone Frustums Computed by Newtonian Impact Theory. NASA TN D-149, 1959.

Figures 1 and 2 are contained in a pocket attached to the back cover of this report.

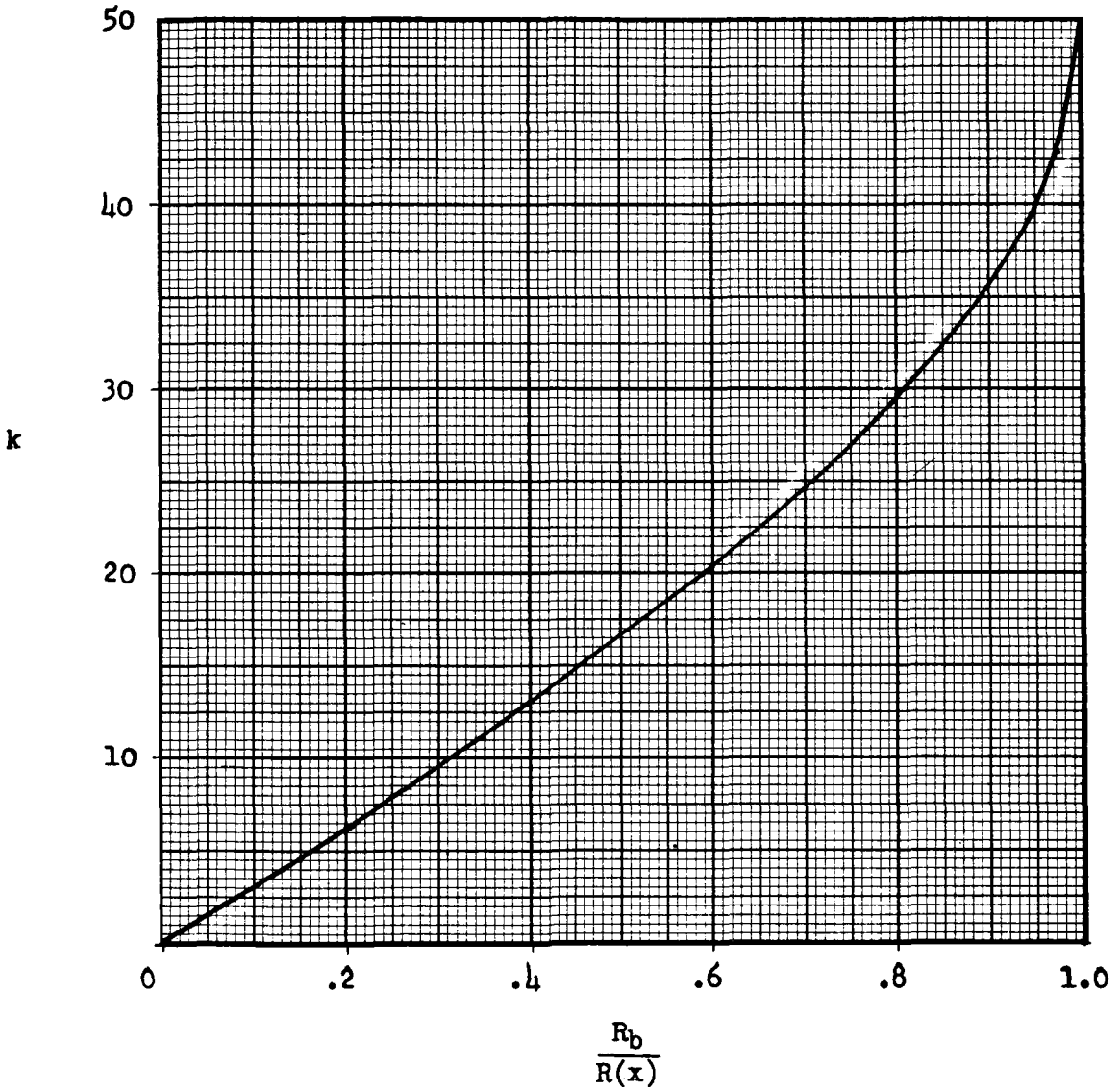

Figure 3.- Variation of the parameter k with the ratio $R_b/R(x)$ where k, the maximum percent shielding due to forebody, is defined by equation (25).

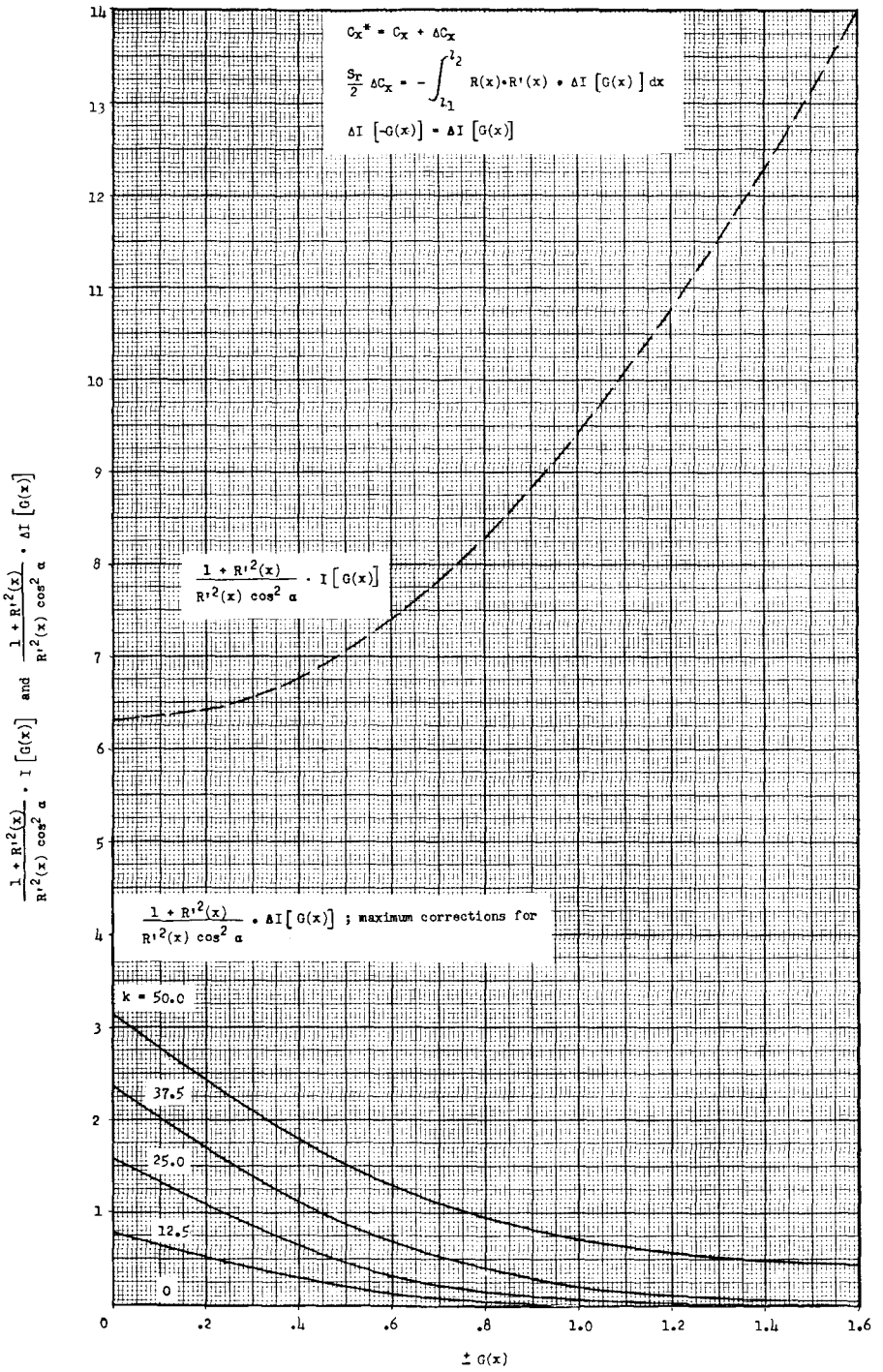

Figure 4.- Chart for evaluation of the function $\Delta I\left[G(x)\right]$.

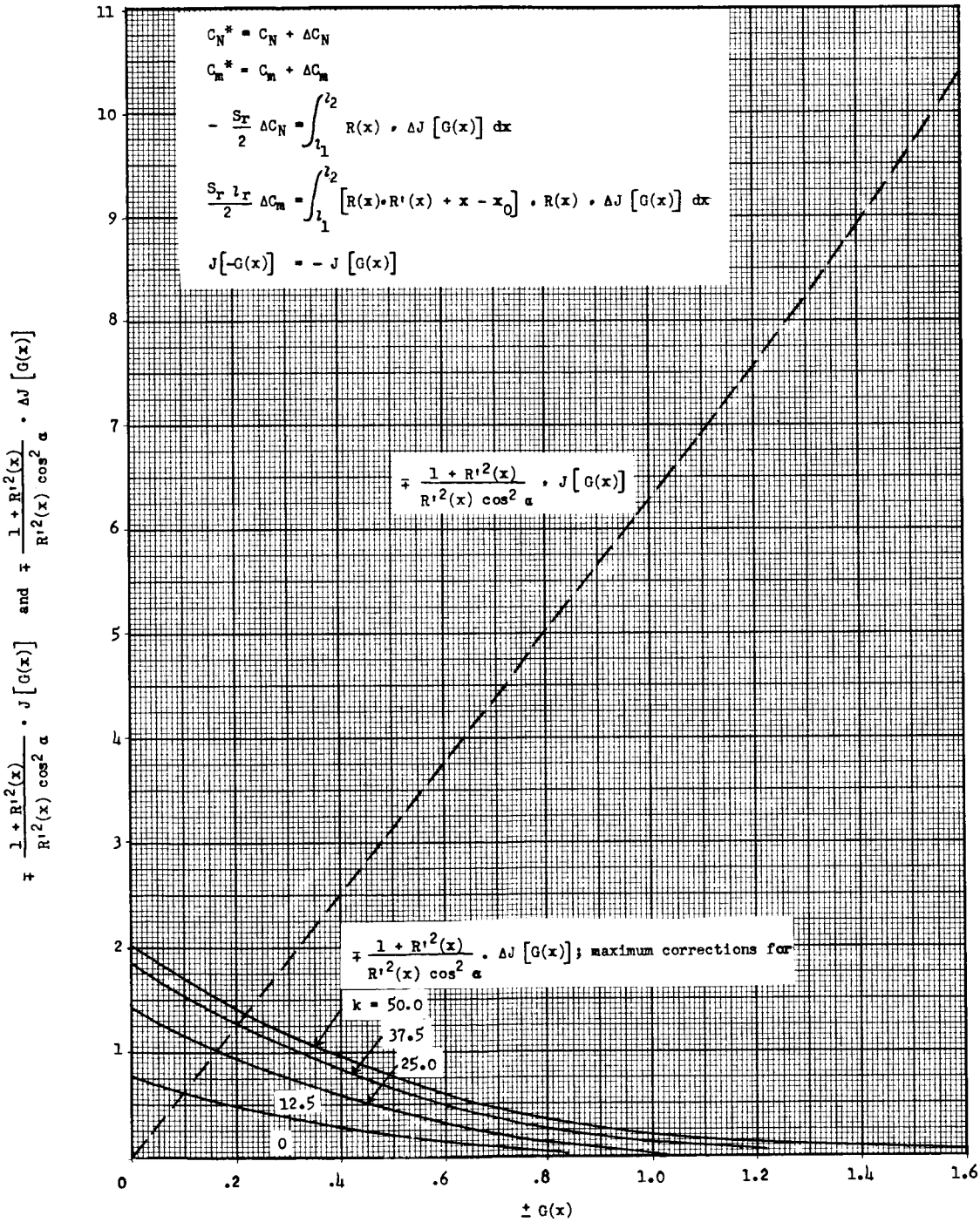

Figure 5.- Chart for evaluation of the function $\Delta J\left[G(x)\right]$.

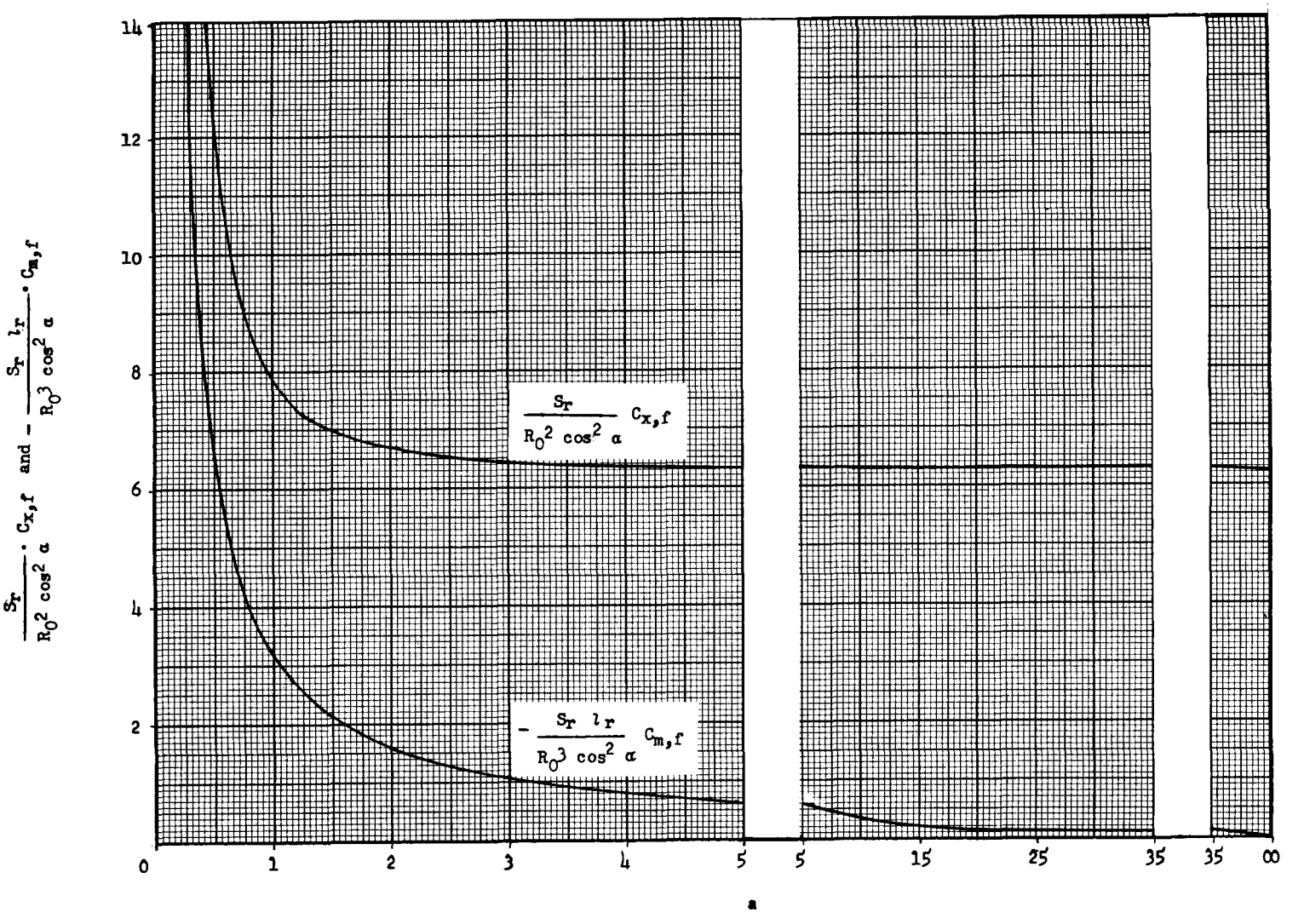

Figure 6.- Chart for evaluation of the force and moment contributions $C_{X,f}$ and $C_{m,f}$.

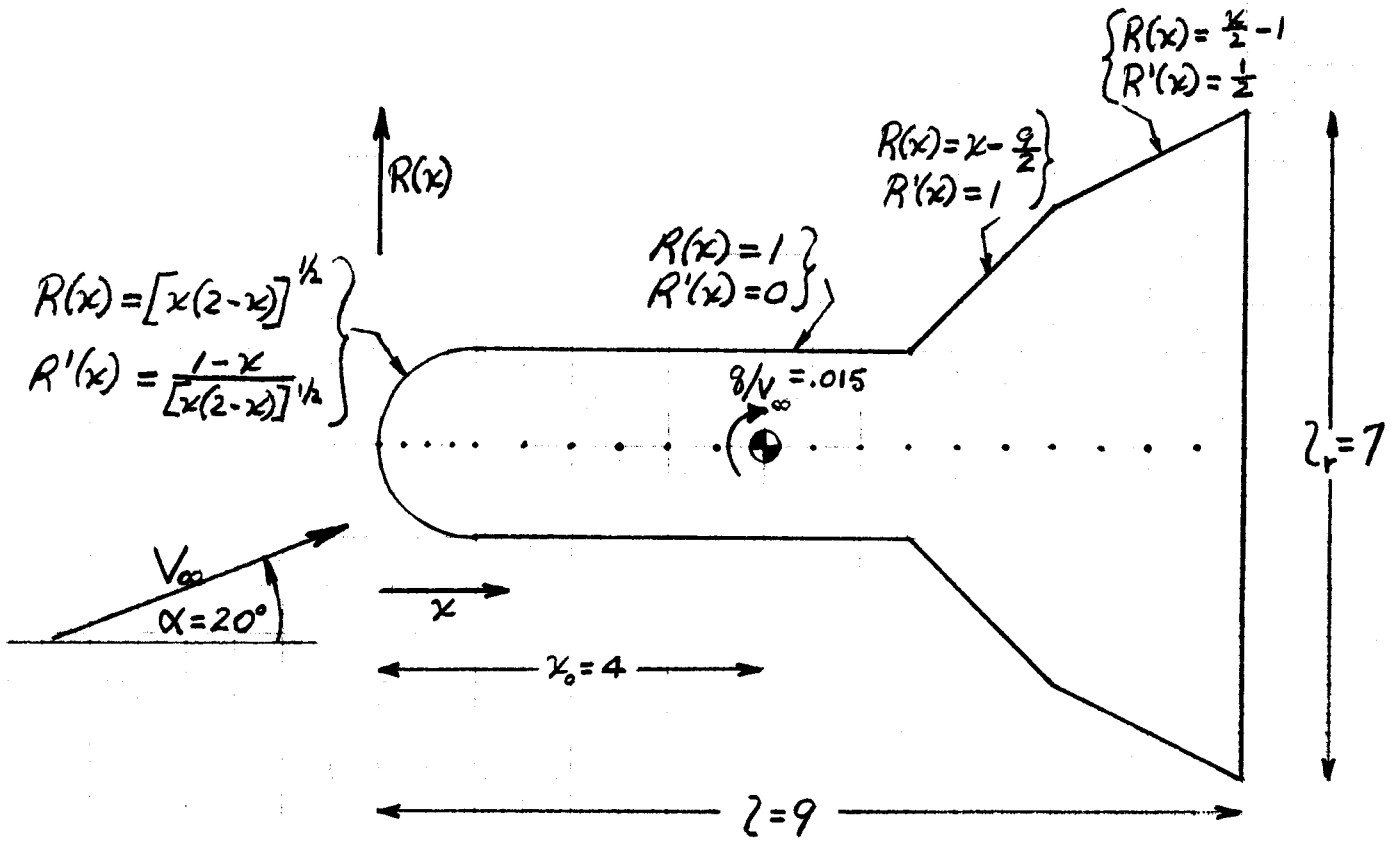

Figure 7.- Body of revolution used to illustrate computational procedures. Note that the reference length and area chosen are $l_r = 7$ and $S_r = \frac{\pi}{4} l_r^2 = 38.48$, respectively.

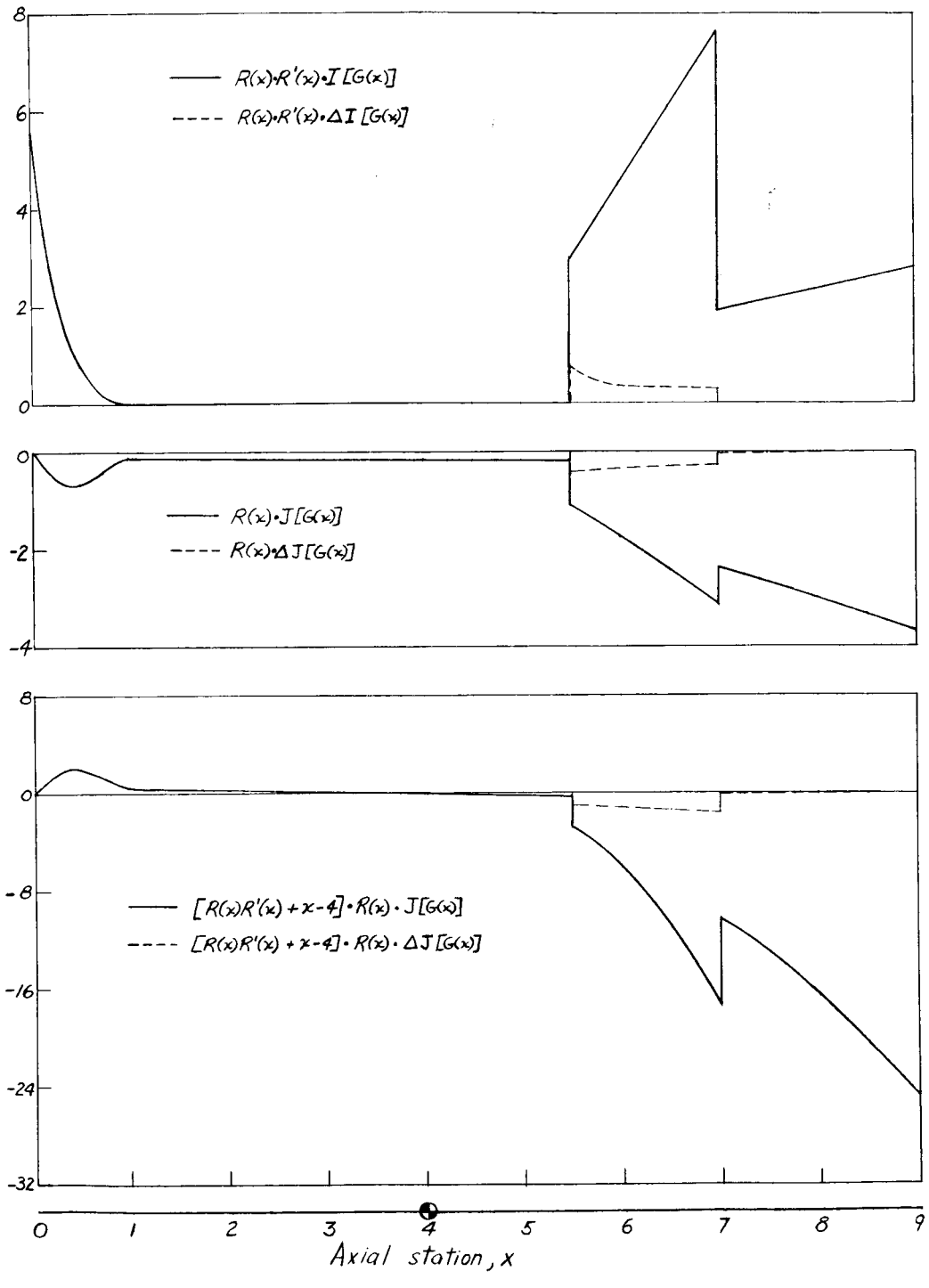

Figure 8.- Axial variations of several functions obtained for body of revolution shown in figure 7.

L-1225